

Investigation of tribological behavior of Diamond-like Carbon coated HSS M2 steel for Hydraulic applications

Keshav M¹, Shanmukha Nagaraj¹, A Bharatish¹

¹Department of Mechanical Engineering RV College of Engineering, RV Vidyaniketan Post Mysore Road Bengaluru-560059

Abstract

Diamond-like Carbon (DLC) coatings are being increasingly adopted in a number of applications, owing to their unique combination of properties, such as high hardness, low wear, and the ability to add various dopants to modify the properties. This research seeks to assess the impact of a DLC coating on HSS M2 steel from the perspective of wear and frictional contact stresses. The study focuses on transient of an ASTM G99 pin-on-disc tribometer test, which constitutes a rotating rigid 20MnCr5 disc against a deformable cylindrical DLC coated pin with a frictional contact between the surfaces. A DLC thin film was deposited on HSS M2 cylindrical pin using PACVD. The characterization of an actual DLC film coated on HSS M2 pin was carried out to determine the properties of the DLC coating, which were provided as inputs to the software. These include SEM imaging, EDS and Nano-indentation. The transient structural mode within ANSYS 18.1 FEA software was adopted for the purpose of the simulation. The obtained hardness and young's modulus of the coating was 17.92 GPa and 230.8 GPa respectively. The FE results shows that the wear volume in the uncoated pin are circa 106% higher than the DLC coated pin, at the highest load condition, and 16.45% higher at the least load condition and the frictional contact stresses for the DLC coated pin versus that of the uncoated shows that the coated pin reduces the frictional stresses by 56.21% on an average for all the load conditions.

Keywords: *DLC, FEM, ANSYS, ASTM G99, Pin on disc tribometer, Archard's Wear Law*

List of Acronym:

DLC: Diamond like Carbon SEM: Scanning Electron Microscopy

EDS: Energy Dispersive Spectroscopy FEM: Finite Element Modelling

PACVD: Plasma assisted chemical vapour deposition

1. Introduction

In recent years, diamond-like carbon (DLC) coatings have gained interest in several applications by the virtue of their distinctive properties such as chemical inertness, high hardness, improved wear resistance, and biological compatibility [1, 2]. DLC coatings are provided on high-speed steel (HSS) tools, punching dies, automobile engines, and biomedical implants [3]. Also, DLC-coated hydraulic components such as vane pumps, piston pumps, and cylinders have attracted the attention of researchers. During the operation of a vane pump, the vane tip slide against the inner surface of the cam ring and their intermittent operation leads to metal-to-metal contact. When the pump operates at lower speed, increase in friction coefficient causes significant wear of the contact surfaces. Hence, the pump performance is considered as a function of friction coefficient between the vane tip and cam ring which is critical for the operation.

Some of the researchers have investigated the effect of DLC coating on the performance of metals and non-metals such as stainless steel, copper, and rubber for various applications. Wu et al. [4] reported the influence of DLC coating on nitrile butadiene rubber. DLC along with the appropriate interlayers was found to reduce the overall coefficient of friction in the rubber wafers.

Jin et al. [5] evaluated the friction performance of DLC/spinel composite coating 304 stainless steel in order to against ZrO₂ in dry sliding condition. The DLC-coated specimen exhibited more stable wear at elevated temperatures when compared to that of as-received stainless steel substrate.

Lu et al. [6] coated a multi-layer DLC film on a soft copper substrate, along with a SiC buffer layer. They noted that the issue of high difference in hardness between the base and coating can be resolved using the appropriate interlayers. This also ensured that the stresses on the DLC coating would be reduced. Further, the functional coating improved the tribological properties of the base material, in addition to increasing of hardness up to 9 GPa.

Łępicka et al. [7] investigated the effect of DLC coating on 316 LVM stainless steel. The DLC coating was worn out by ploughing induced by small patches of the film detached from the substrate. The average coefficient of friction and critical load was found to be 0.15 and 10.65 N, respectively.

Duminica et al. [8] investigated the effect of chromium and chromium nitride interlayer on the adhesion of DLC films deposited on stainless steel. Lower sliding wear rate of DLC films around 3×10^{-17} m²/N was achieved with friction coefficient below 0.1 with improved durability. Kim and Kim [9] investigated the effect of sliding velocity (0.01–0.04 m/s) and ambient temperature (27–160°C) on the wear rates of DLC-coated AISI 52100 steel balls. The friction and wear decreased with the increase in sliding velocity due to the decrease in surface asperities. With an increase in temperature, due to increase in degree of graphitized worn DLC coatings, friction coefficients decreased with the increase in wear rate. Ma et al. [10] developed a mathematical model for the normal force exerted by the vanes on the cam rotors and total disturbing torque induced on the cam rotors. Increase in friction coefficient between the vane and the slot leads to the increase in torque fluctuation of vane motor. The normal force decreased with the increase in the friction coefficient. Inaguma and Hibi [11] investigated the effect of friction torque characteristics on the mechanical efficiency of the vane pump. Decrease in the friction coefficient of the vane tip contributed to the improvement of mechanical efficiency. Inaguma [12] also reported that DLC-coated vane tips decreased the friction torque, by smoothing the surface of the cam contour. Ashmawy and Murrenhof [13] reported the effect of relative speed between the vane tip and cam ring, normal vane force, pressure difference between two sides of the vane and vane tip coating material on friction coefficient of vane tip and cam ring interface. To reduce the friction, the relative speed between vane tip and cam ring was to be higher than 4.8 m/s. The effect of normal vane force and pressure difference and coating material were less significant.

To reduce the efforts of tribological experimentation, some of the researchers have developed the simulation models to understand the behavior of various materials subjected to wear and friction. Pandure et al. [14] have developed finite element model to predict nanoindentation response of DLC-coated HSS steel and validated the same through experiments. At small indentation depths, the plastic deformation took place around the ball indenter tip and propagated in both vertical and lateral directions at smaller indentation depths. Suresh et al. [15] modeled the wear depth and contact pressure of Al 6061 metal matrix composite, using finite element analysis. The wear coefficient was experimentally determined and was correlated with the wear depth obtained in the simulation. For 50 N load, a wear depth of 3.38E–04 m was obtained and the contact pressure of 2.088 MPa was obtained. Deviation of simulation results from experimental was found to be 7.3%.

Holmberg et al. [16] performed finite element analysis to analyze the stresses generated due to sliding spherical counter face of DLC- and TiN-coated elastic-plastic steel. While the maximum tensile stress on the top surface of the DLC coating was about 900 MPa, TiN coatings exhibited higher tensile stress of 3000 MPa.

Li [17] developed a numerical model for pin and disk interaction which simulates the friction and wear conditions on the rake face of a metal cutting tool. The authors reported that the rotation of the pin will introduce a frictional shear stress at the surface due to which von Mises stress increases and causes plastic deformation at the pin tip contact region.

Söderberg and Anderson [18] predicted wear of the pad and rotor contact by performing structural analysis using ANSYS finite element code. The deepest wear occurred in the region of high pressure and asymmetrical pressure distribution resulted in a longer running – in process.

There have been numerous experimental studies reported on the effect of friction and wear parameters on the performance of DLC-coated steel substrates incorporating various inter-layers such as chromium and chromium nitride. Some of the researchers have also developed the mathematical models for uncertain output of interest such as normal force exerted on the vanes and total fluctuating torque on vane motor. Since the experimental wear testing of DLC-coated steel substrates is very expensive and time consuming, a simple numerical model is required for analyzing the hard-coated steel pins and disk interaction under dynamic

conditions. Also, performance of DLC-coated vanes for hydraulic applications needs to be explored extensively. Hence, this paper aims at developing a numerical model for the interaction of DLC-coated HSS M2 steel pin with 20MnCr5 case hardened steel disk to simulate the behavior of vane tip sliding against the inner surface of the cam ring. Transient structural analysis was performed to investigate the effect of normal load on the wear volume, frictional stress, contact pressure, total deformation, vonMises stress, and shear stress responses at ambient temperature. The properties such as elastic modulus and hardness were measured using nanoindentation method and considered as inputs for simulation.

2. Material and methods

2.1 Simulation of interaction of DLC-coated HSS M2 steel with 20MnCr5 disk

The modeling of disk and pin was performed using design modeler of ANSYS 18.1. An 8-mm-thick disk having 165 mm outer diameter and 105 mm inner diameter was modeled. A pin of 10 mm diameter and 30 mm height was modeled containing two interfaces—2.5- μm -thick DLC thin film and 29 mm HSS M2 steel. The “add frozen” operation was adopted to define different material interfaces to pin. The pin was positioned at a distance of 67.5 mm from the center of the disk. The properties of HSS M2 and 20MnCr5 were referred from the material datasheet. The elastic modulus of DLC obtained from nanoindentation was given as one of the inputs. The properties of DLC, HSS M2 steel, and 20MnCr5 steel are as shown in Table 1.

Table 1 Properties of materials

Material	Property	Value
DLC	Young's modulus (Pa)	2.308E+11
	Poisson's ratio	0.22
	Density (kg/m^3)	2500
HSS M2	Young's modulus (Pa)	2.18E+11
	Poisson's ratio	0.3
	Density (kg/m^3)	8160
20MnCr5	Young's modulus (Pa)	2.05E+11
	Poisson's ratio	0.29
	Density (kg/m^3)	7850

The disk target and contact pin are depicted in Fig. 1. The coefficient of friction was set to 0.1 which accommodates the surface roughness at the contact region. The asymmetric behavior to determine the wear on the contact surface was adopted along with nodal-normal detection method. Augmented Lagrange formulation was performed as it adds additional control to automatically reduce penetration. A command script was used for determining the wear volume of the DLC pin.

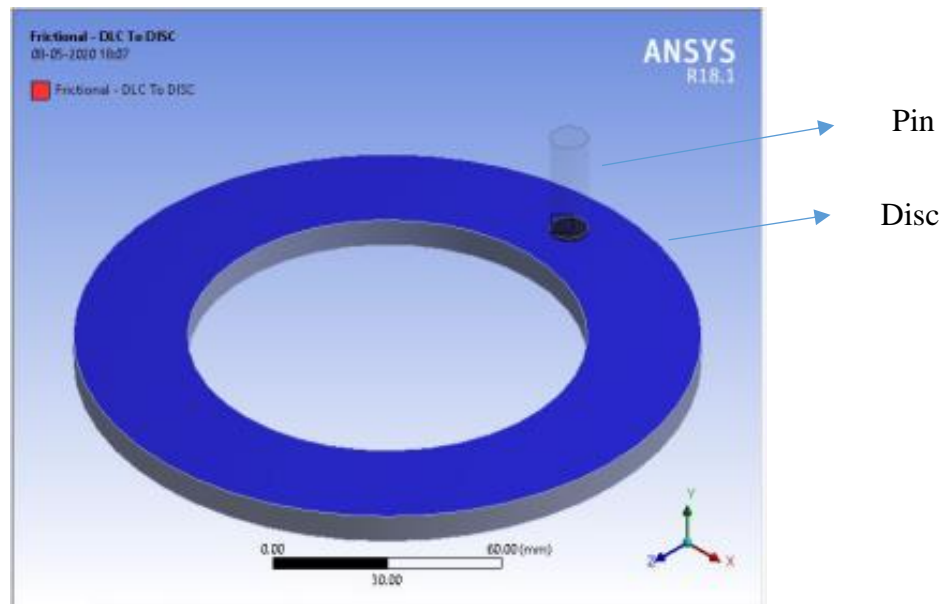


Fig. 1 Target and contact bodies

The model was discretized using ANSYS Workbench 18.1. The element size was considered as 3 mm. The mesh was refined at critical area to improve the accuracy of the results. The element size at contact region was set at 1 mm. Fig. 2a shows the meshed model of pin and disk interaction. For analysis purpose, CONTA174 elements were used for contact body and TARGE170 elements were adopted for target body. The average aspect ratio obtained was 1.5523 and average element quality was 0.88 which indicated that the obtained mesh quality was reasonably good. To incorporate the surface changes due to material loss, “mesh nonlinear adaptivity” was utilized for remeshing the contact surfaces. The number of elements and nodes obtained for disk were 3376 and 7034, respectively, and those of pin were 2951 and 1767, respectively. For the given model, boundary conditions were defined using two joints, namely, the revolute and translational. The revolute joint was defined for the purpose of enabling rotation to the disk as shown in Fig. 2b. In the local coordinate system, the translation motion in X , Y , and Z directions was constrained. The rotation was constrained in X and Y directions. The translational joint was defined to enable the displacement of the pin as indicated in Fig. 3a. Except for the displacement in the X direction, all other motions of the pin were restricted. The load range on the pin was selected as 20–180 N based on pressure acting under the vane in a hydraulic pump and was applied on the vane as shown in Fig. 3b. A contact tool was used to determine contact stress and frictional stress at the contact region.

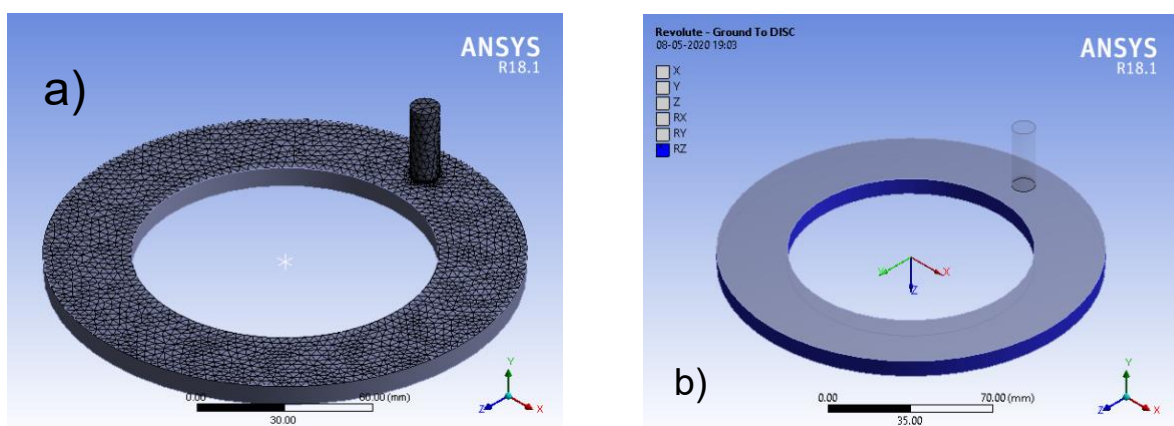


Fig. 2 (a) Meshed model and (b) revolute joint

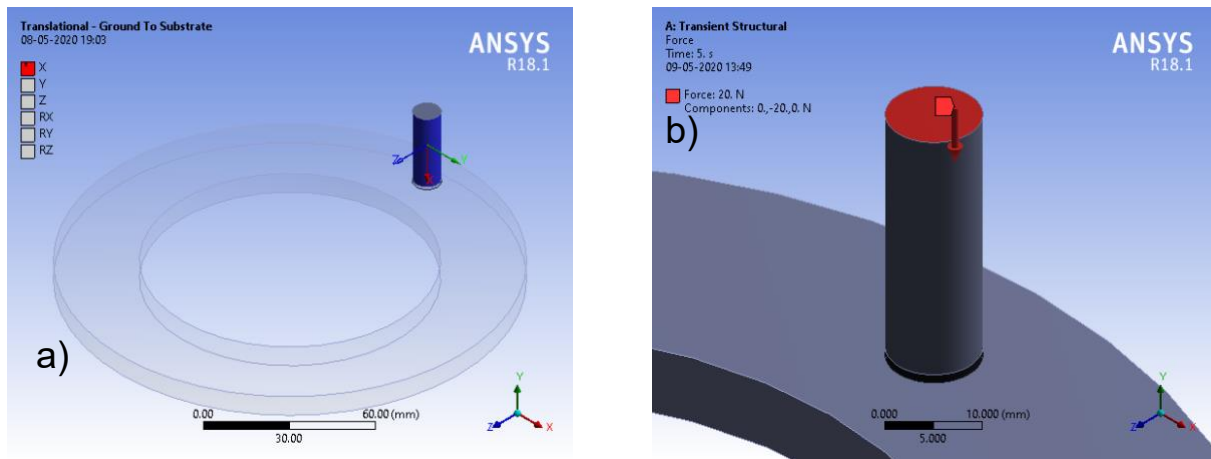


Fig. 3 (a) Translation joint and (b) force applied on pin

3. Result and Discussion

3.1 The effect of normal load on wear volume of DLC-coated HSS M2 steel pin

The variation of wear volume of DLC-coated and -uncoated HSS M2 pin with respect to the varying normal load is as shown in Fig. 4. In general, it was observed that wear volume increased with the increase in normal load for both DLC-coated and -uncoated HSS M2 pins. The wear loss was nearly negligible at lower values of load for both DLC-coated and -uncoated HSS M2 Pin. The wear volume obtained at 20 N was 0.0005968 mm³ for DLC coatings and as-received HSS M2 was 0.000695 mm³. At 180 N of normal load, wear loss was obtained as 0.0010288 mm³ for DLC coatings and that for as-received HSS M2 was 0.0021198 mm³. It can also be noted that the wear volume drastically increased from 0.001109 to 0.0021198 mm³ when the load was increased from 100 N to 180 N, respectively, for HSS M2 coating. This was mainly due to progressive destruction of material that results from ploughing action caused by hard and detaching wear debris from HSS M2 surface layer. On the other hand, lower wear volume was observed for DLC-coated HSS M2 at higher loads. This can be attributed to lower elastic modulus mismatch between the substrate and coating [$E_{\text{substrate}}/E_{\text{coating}}=0.94$] which in turn improves the wear resistance of steel due to DLC coating. This is in accordance with Oliver et al. [19].

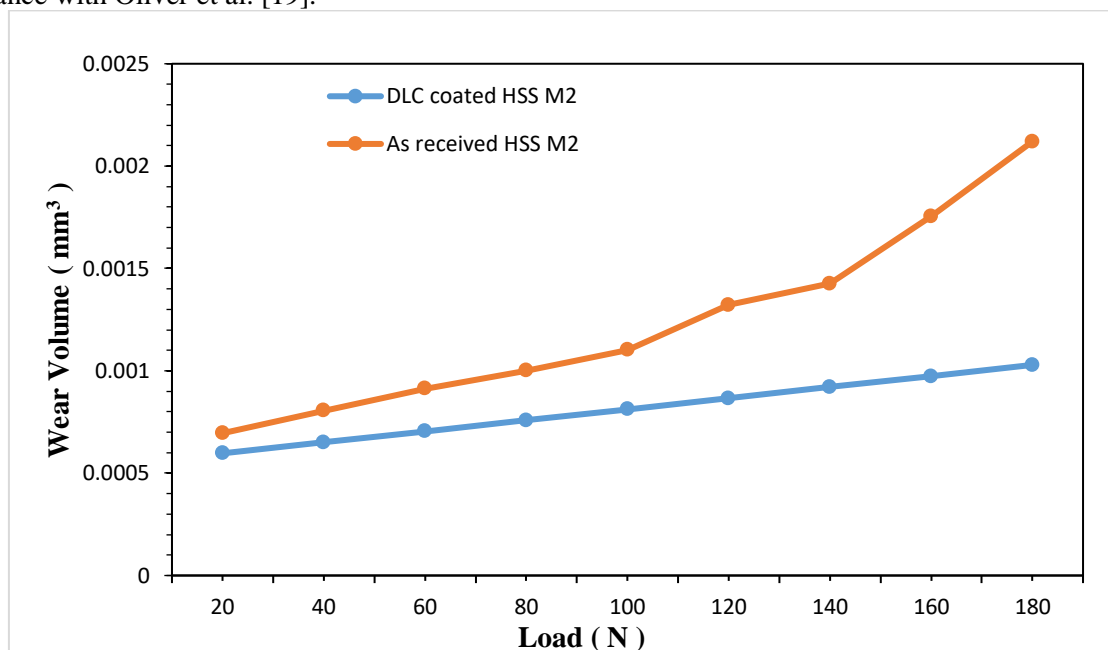


Fig. 4 Variation of wear volume of DLC coatings and HSS M2 steel with normal load

3.2 Contact pressure

The contact pressure was evaluated for every substep of analysis at the interface of the pin and disk. The contact pressure was found to be correlated linearly with normal load applied on the surface of pin. Fig. 5(a) predicts the distribution of contact pressure in DLC-coated HSS M2 pin and Fig. 5(b) shows the variation of contact pressure along the diameter of the pin. The effect of lower normal loads on contact pressure of both DLC-coated and HSS M2 pin was not found to be significant. However, at higher normal load of 180 N, maximum contact pressure of 7.008 MPa was found for HSS M2 pin and 6.152 MPa for DLC-coated HSS M2. This decrease in contact pressure can be attributed to the possible reduction of heat generation at the interface because of enhanced heat dissipation by DLC coating during interactive sliding process as indicated by Gabriel et al. [23]. Also, decrease in contact pressure reduces the combined effect of compressive and shear stresses on the coating and hence improves the life of the coating as demonstrated by Mishra et al. [24].

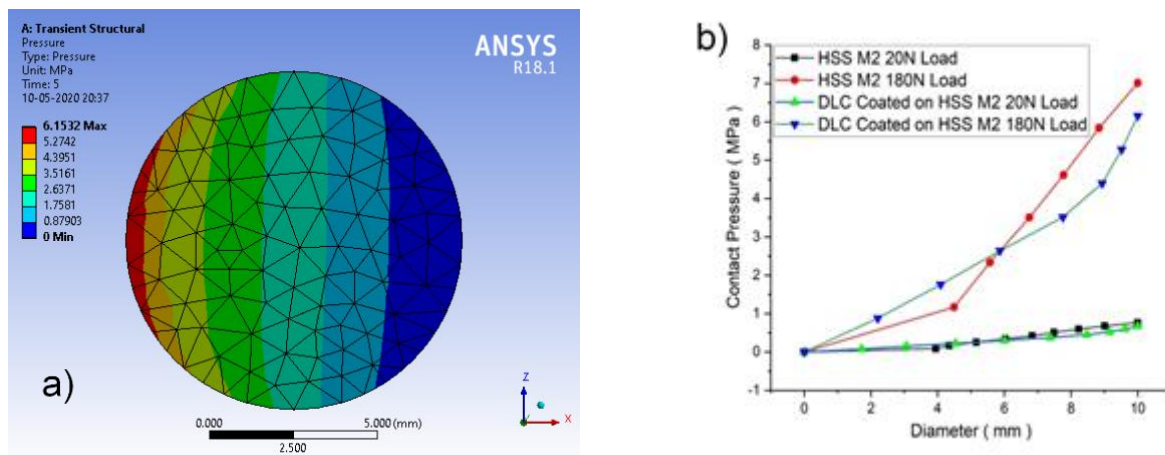


Fig. 5 (a) Contact pressure for DLC-coated HSS M2 at 180 N load and (b) variation of contact pressure along the pin diameter

3.3 Frictional stress

Frictional stress is a function of contact pressure. A contact tool was used to determine the frictional stress at the defined contact region. The variation of frictional stress along the diameter of the pin is as shown in Fig. 6(a). From the obtained results (Fig. 6(b)), it was observed that the frictional stresses developed on DLC-coated pin got decreased when compared to that of HSS M2 pin. At 20 N, there was no significant difference in induced frictional stress for DLC-coated HSS M2 and HSS M2 pins. However, at higher loads of 180 N, greater reduction of frictional stresses (around 56%) was achieved when DLC coatings were employed. This may be due to higher degree of graphitization which causes reduction in shear resistance of contact asperities [25]. The maximum frictional stress obtained for DLC-coated pin was 0.615 MPa.

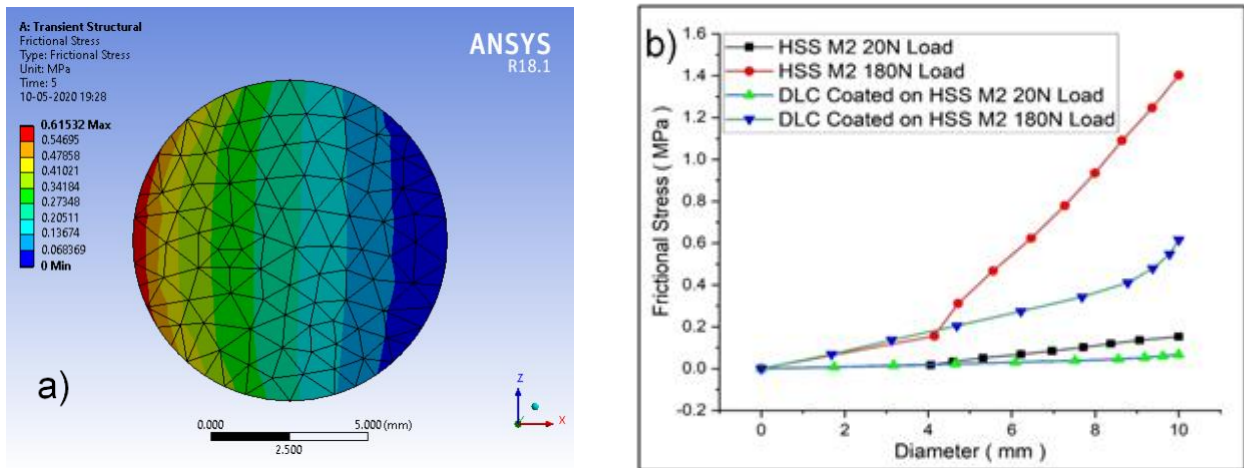


Fig. 6 (a) Frictional stress for DLC-coated HSS M2 at 180 N and (b) variation of frictional stress along the pin diameter

3.4 Von Mises stress, shear stress, and deformation

The variation of vonMises stress from trailing to leading edge with increasing load is as shown in Fig. 7(a) and (b). Considering leading edge, maximum vonMises stress of 5.84 MPa was found at 180 N applied on HSS M2. With the application of DLC coating, reduction in the stress was achieved from 5.84 MPa to 5.45 MPa. However, on the trailing edge, maximum von Mises stress of 7.492 MPa was observed at 180 N applied on HSS M2 and the same got reduced to 4.849 MPa with the application of DLC. There was no significant change in stress levels observed at lower load of 20 N for both DLC-coated HSS M2 and HSS M2. The von Mises stress contours in trailing and leading edge of pin as shown in Fig. 7(a) and (b). Front and back views are shown in Fig 8, 9, 10 and 11 for 20 N and 180 N loads. The deformation levels of DLC at 180 N was also found to be significantly reduced when compared to that of as-received HSS M2 as indicated in the contour plot of deformation and variation of load with deformation in Fig. 13(a) ,14 and 13(b). When the DLC film is very thin, the effect of ploughing is very small and causes lower level of deformation of DLC. Since the friction of thin film of DLC sliding against disk is also determined by the shear strength, the shear stresses were analyzed and the shear stress contour is as shown in Fig. 15, 16 and variation with load in Fig. 17. At higher loads, the shear stress also got reduced due to DLC coating since DLC had good ability to develop a surface with low resistance to shearing [22].

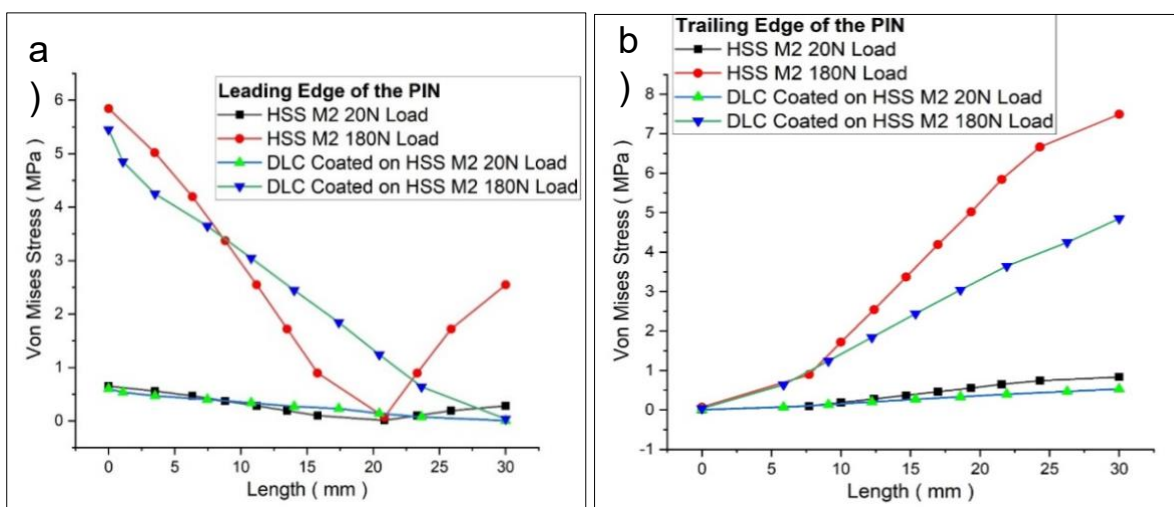


Fig. 7 Variation of von Mises stress along the pin diameter at (a) leading edge and (b) trailing edge

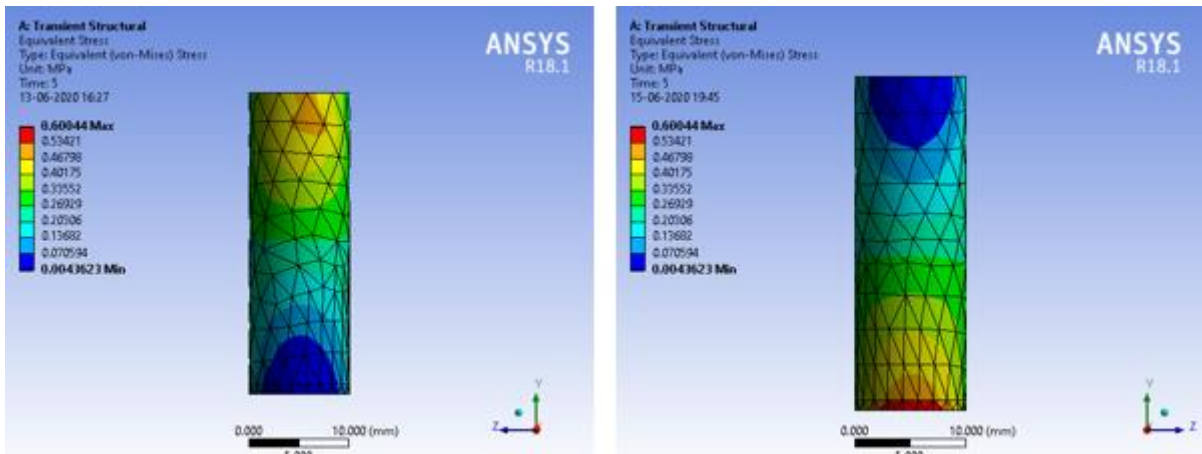


Fig 8 a) Front and b) Back view of Von mises stress contour for DLC coated HSS M2 at 20N load

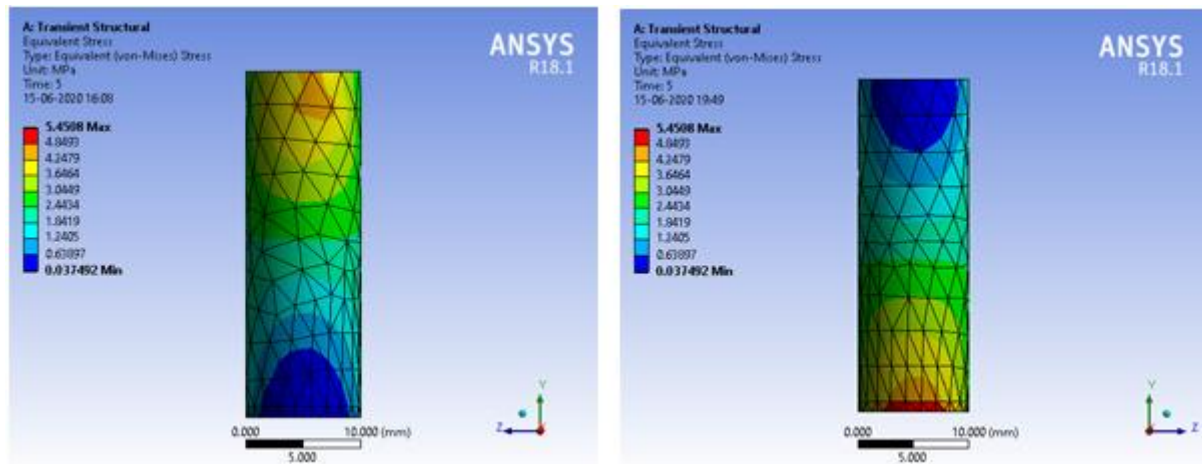


Fig. 9 a) Front and b) Back view of Von mises stress contour for DLC coated HSS M2 at 180N load

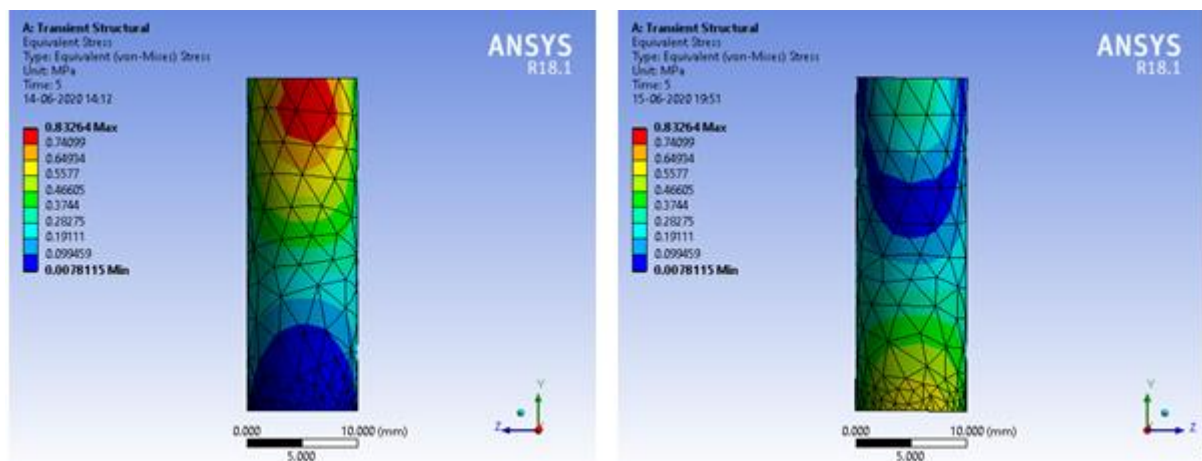


Fig.10 a) Front and b) Back view of Von mises stress contour for as received HSS M2 at 20N load

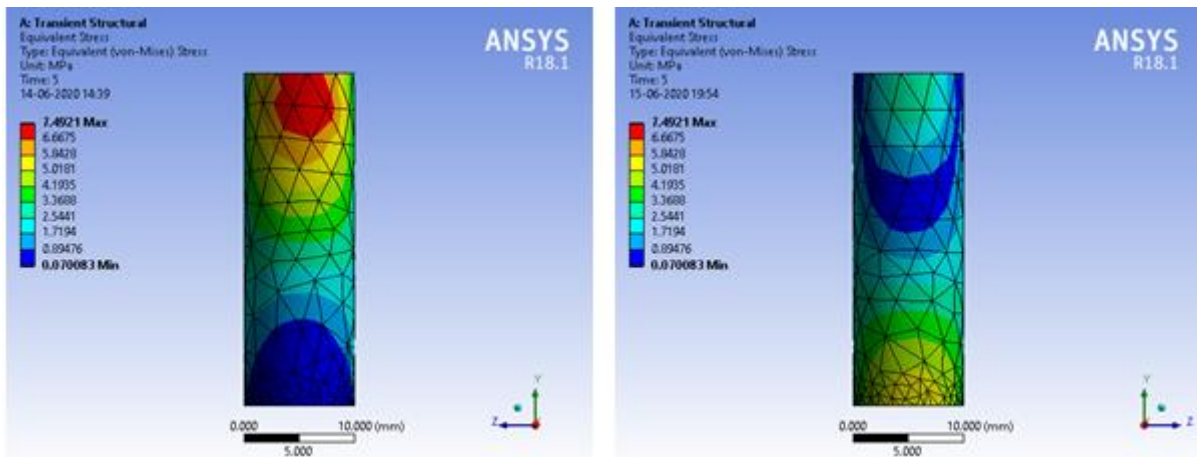


Fig. 11 a) Front and b) Back view of Von mises stress contour for as received HSS M2 at 180N load

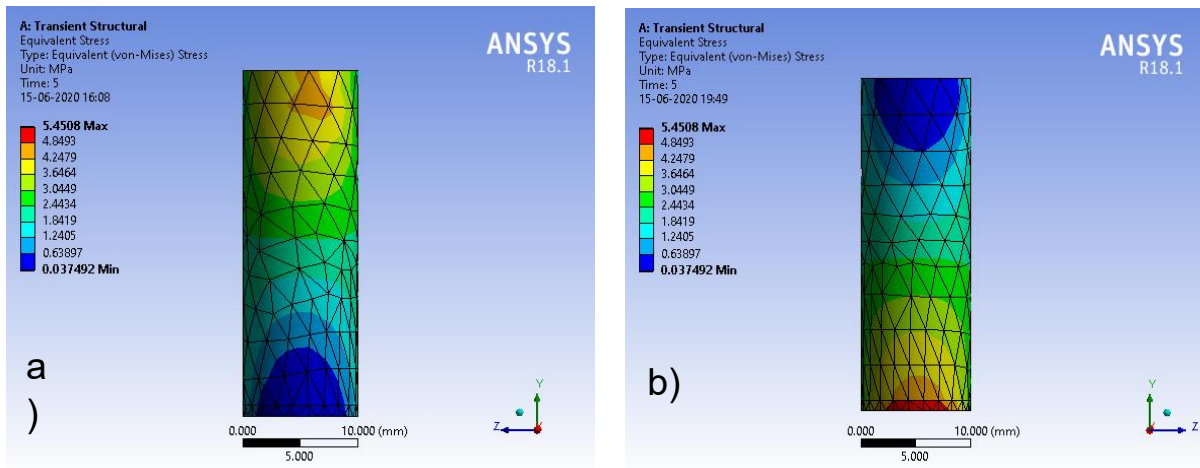


Fig. 12 (a) Leading edge and (b) trailing edge view of von Mises stress contour for DLC-coated HSS M2 at 180 N load

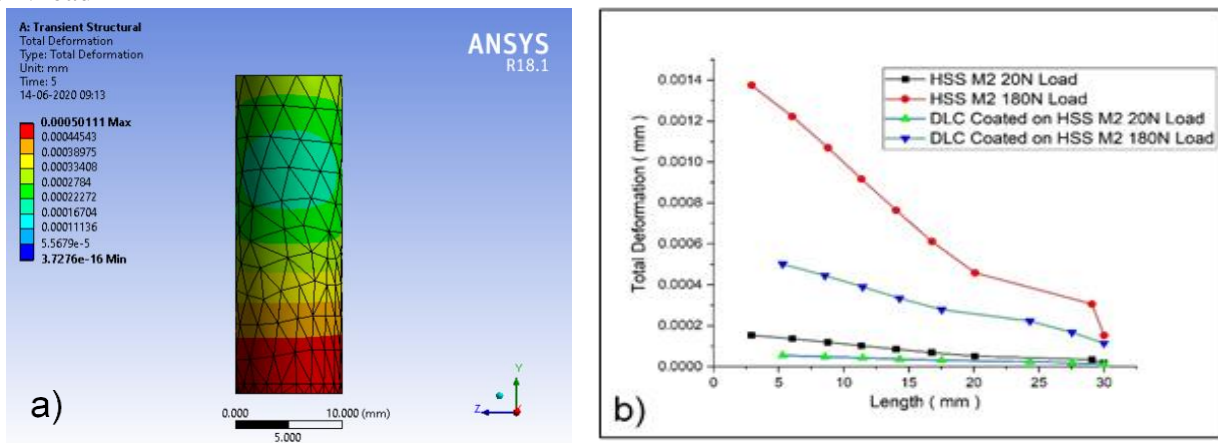


Fig.13 (a) Total deformation for DLC-coated HSS M2 at 180 N load and (b) variation of deformation of pin along its length

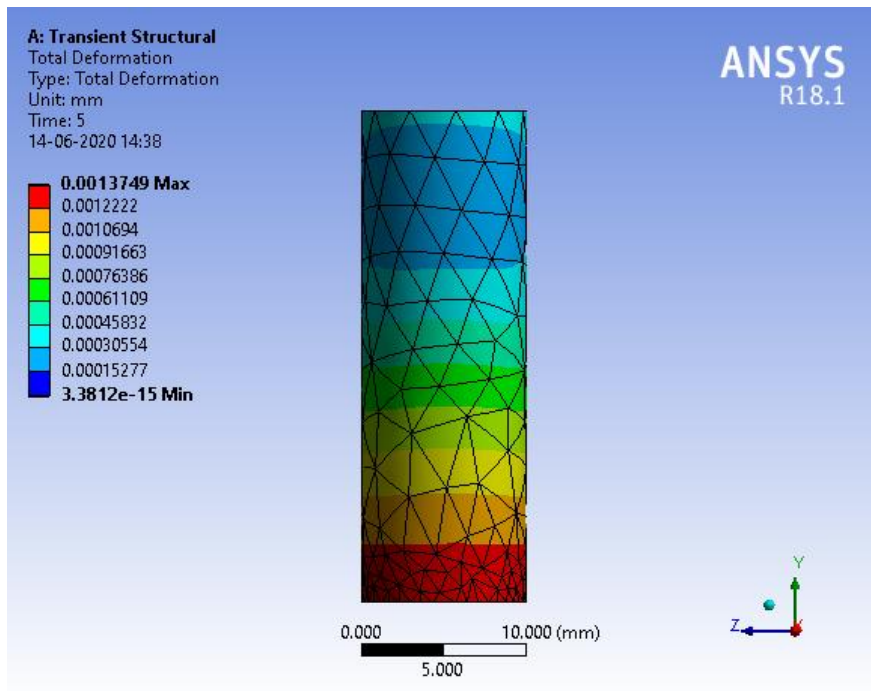


Fig 14 Total deformation for as received HSS M2 at 180N load

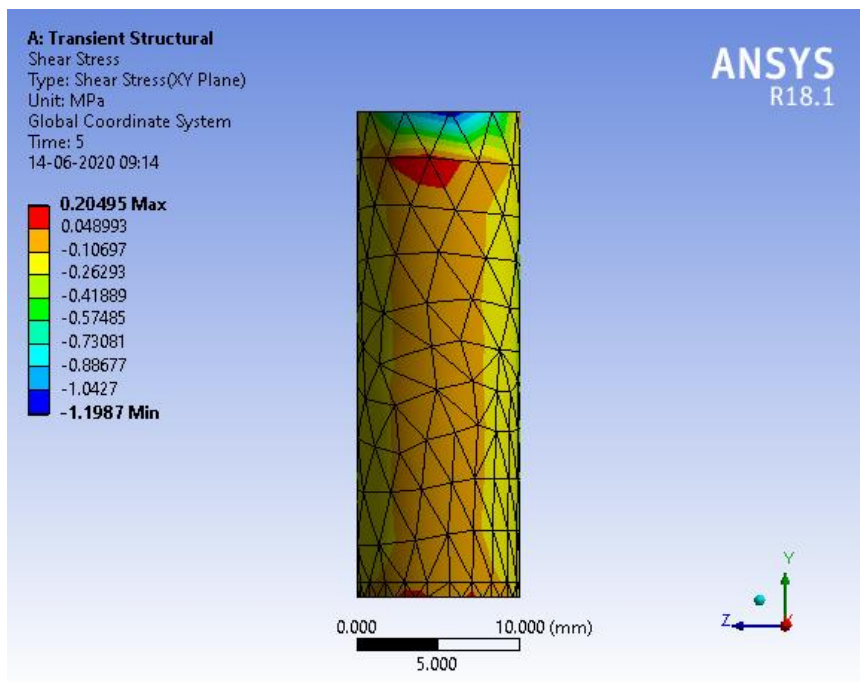


Fig. 15 Shear stress contour for DLC-coated HSS M2 at 180 N load

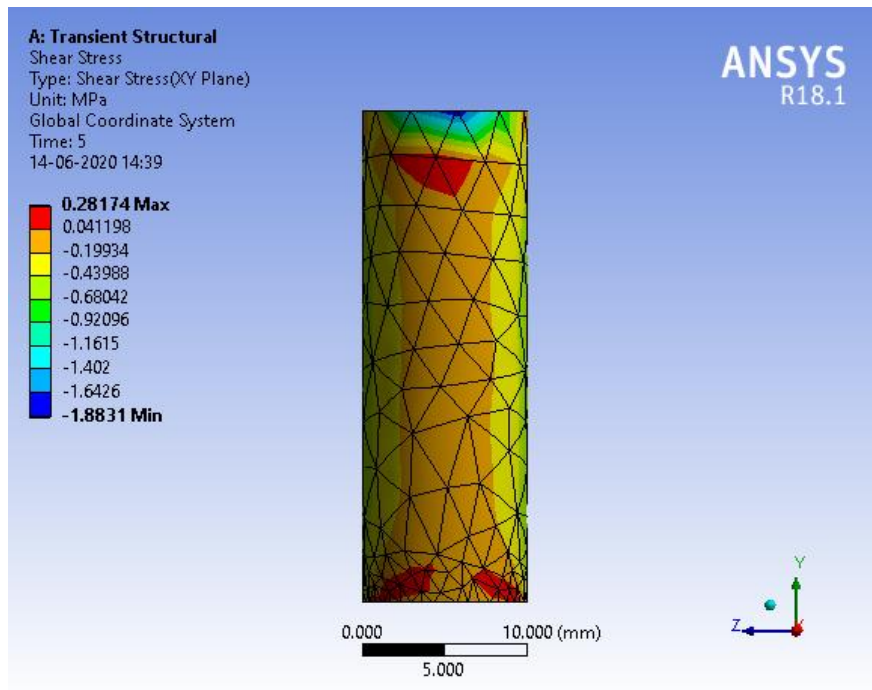


Fig. 16 Shear stress contour for as received HSS M2 at 180N load

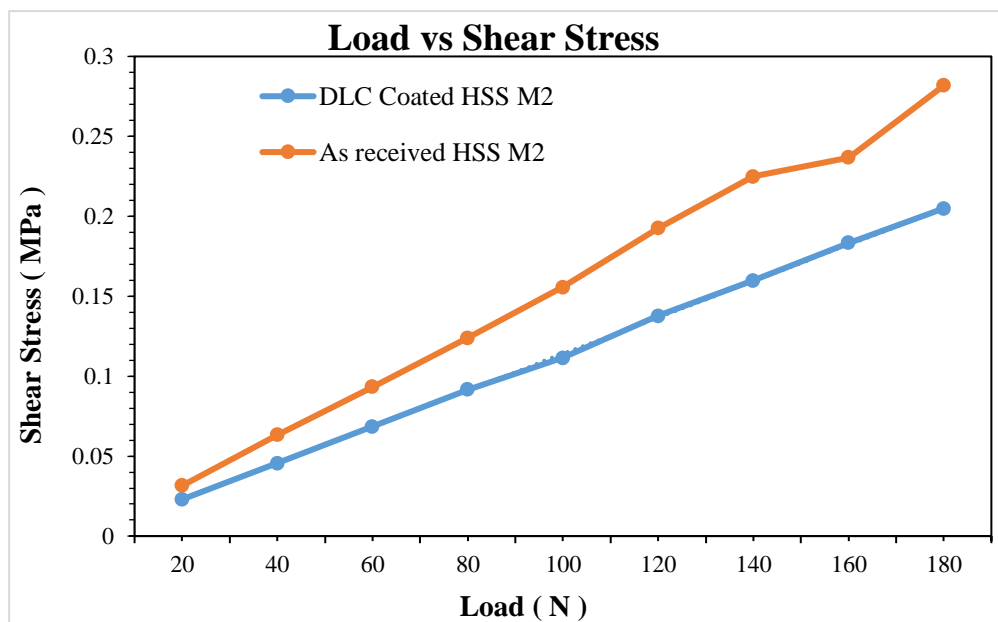


Fig. 17 Variation of shear stress with applied load

3.5 Measurement of mechanical and structural properties of DLC coatings

The hydrogenated DLC thin film was deposited on cylindrical pin of HSS M2 material using a plasma-assisted chemical vapor deposition process at 250 V bias voltage. The thickness of the coating achieved was around 2 ± 0.2 μm . The deposition of DLC was done at 13.56 MHz radio frequency power, 1×10^{-6} mbar chamber pressure, and room temperature. The total gas flow rate was 100 sccm. Acetylene gas was used as a source of carbon and hydrogen.

3.5.1 Scanning Electron Microscope

Scanning electron microscope was adopted to analyze the microstructure, defects, and voids. Surface images of the as-deposited DLC coating were taken using scanning electron microscopy at different magnifications, i.e 200x (Fig. 18 a), 1000x (Fig. 18b) and 2000x (Fig.18c). The SEM was carried out to understand the microstructure, defects and voids. From the SEM image in Fig. 18a, it is observed that the surface of DLC is smooth, continuous and densely packed. A carbon spot is observed on the surface, in Fig. 18c, which is created due to the accumulation of carbon at a particular location on the substrate. For a randomly sampled view field of approximately 1 mm² (at 200 x magnification), there are only two spots visible, and hence it can be concluded that the surface is largely free from defects. Further, the presence of cracks or other deformities are not visible within the given SEM images, on the as-deposited DLC coatings. The surface was largely free from defects and the presence of cracks or other deformities on the as-deposited DLC coating

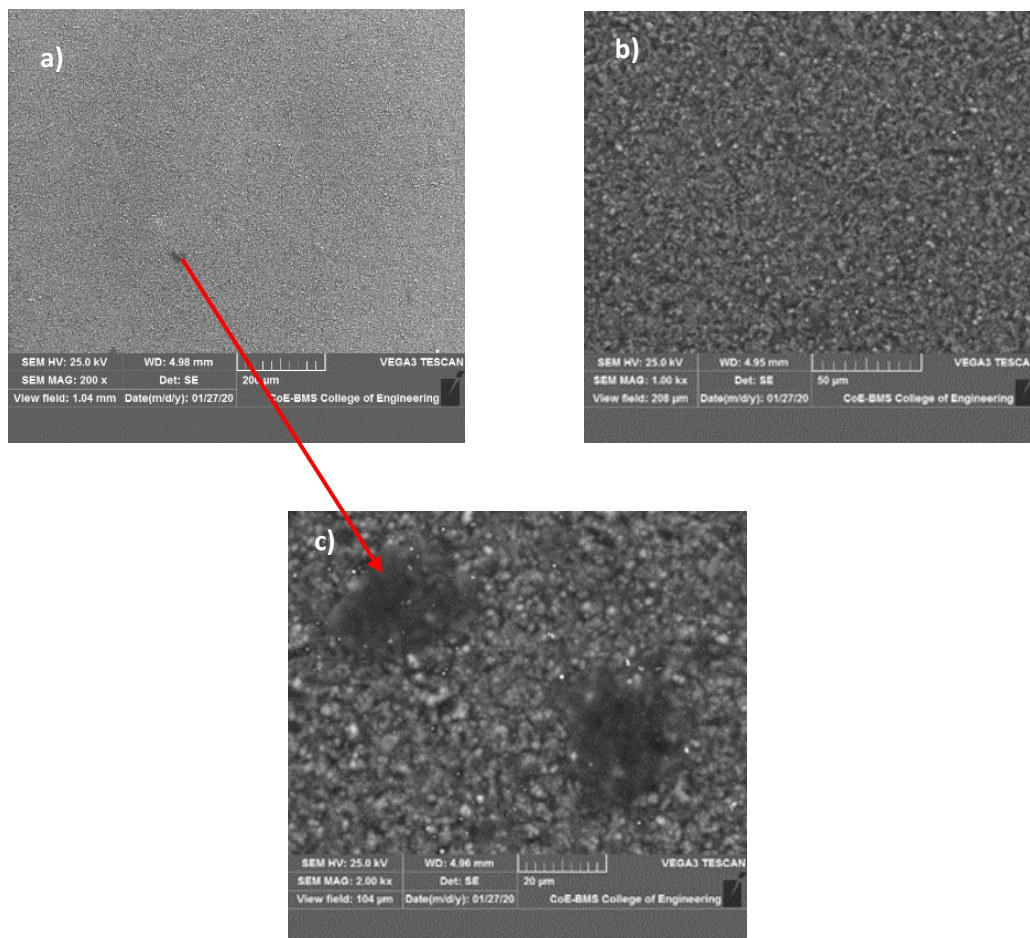


Fig. 18 Microstructure of DLC a) 200x Magnification b)1000x Magnification c) 2000x Magnification

3.5.2 Hardness and Elastic Modulus

Nanoindentation was performed to determine hardness and elastic modulus of DLC coating using Agilent G200 Nanoindenter with a Berkovich indenter tip. A typical load – displacement curve obtained from nano-indenter for DLC coated steel substrates at 250 V of bias voltage and 100 sccm of acetylene flow rate is as shown in Figure.19.

In nano-indentation process, the hardness and Elastic modulus were computed using method introduced by Oliver and Pharr [19]. Hardness is computed by Eq (1).

$$H = \frac{P_{max}}{A_p} \quad (1)$$

where P_{max} is the maximum load and A_p is the projected area of the contact at maximum load given by Equation (2)

$$A_p = 24.56 h_c^2 \quad (2)$$

Where h_c is the contact indent depth considered as the value at the end point of the tangent drawn to load displacement curve. The elastic modulus is computed by finding the slope of the tangent fit to the unloading curve as given by Equation (3)

$$E = \left(\frac{dP}{dD} \right)_{D=D_{max}} \quad (3)$$

It is observed that the relaxation in elastic strain within the material had a strong elastic recovery of 71%, with 29% plastic deformation. Thus, hard DLC coatings were obtained [19]. Also, the mean value of elastic modulus was obtained as 305.6 GPa, From the curve, it is observed that the mean hardness of the coating was 28.8 GPa. The results obtained from the nanoindentation test are as shown in Table 2. The values were stable in the range of 200–300 nm displacement. For every test, the average value of the hardness and elastic modulus for a displacement range of 200–300 nm was computed Youngs modulus vs displacement curve and hardness vs displacement curve is as shown in Fig 20 and Fig 21 for as deposited DLC coated steel..

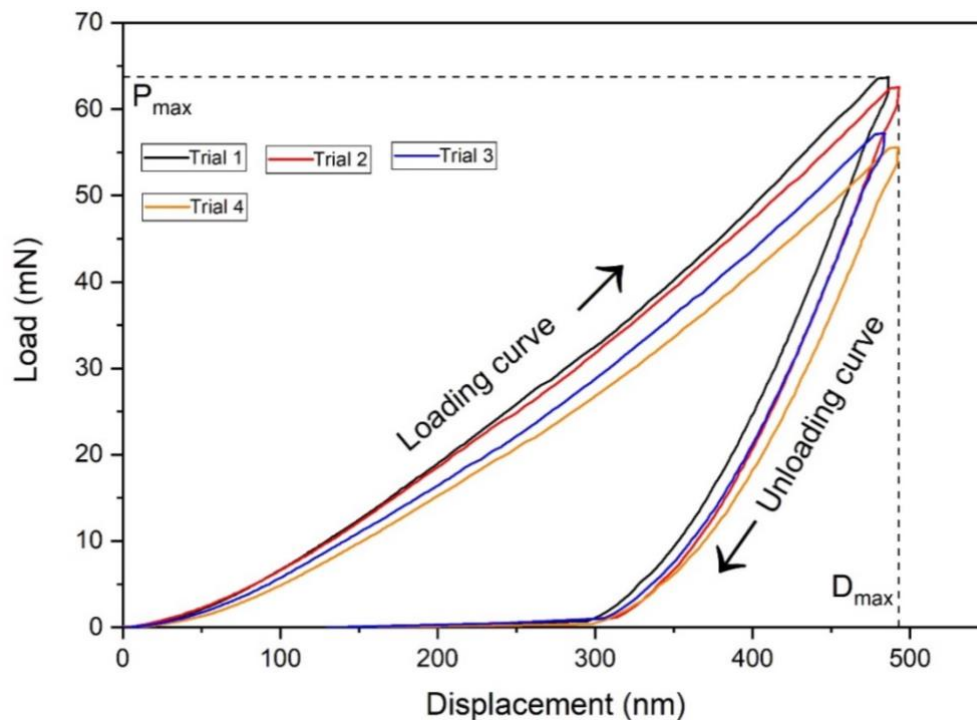


Fig. 19 Load versus displacement curve

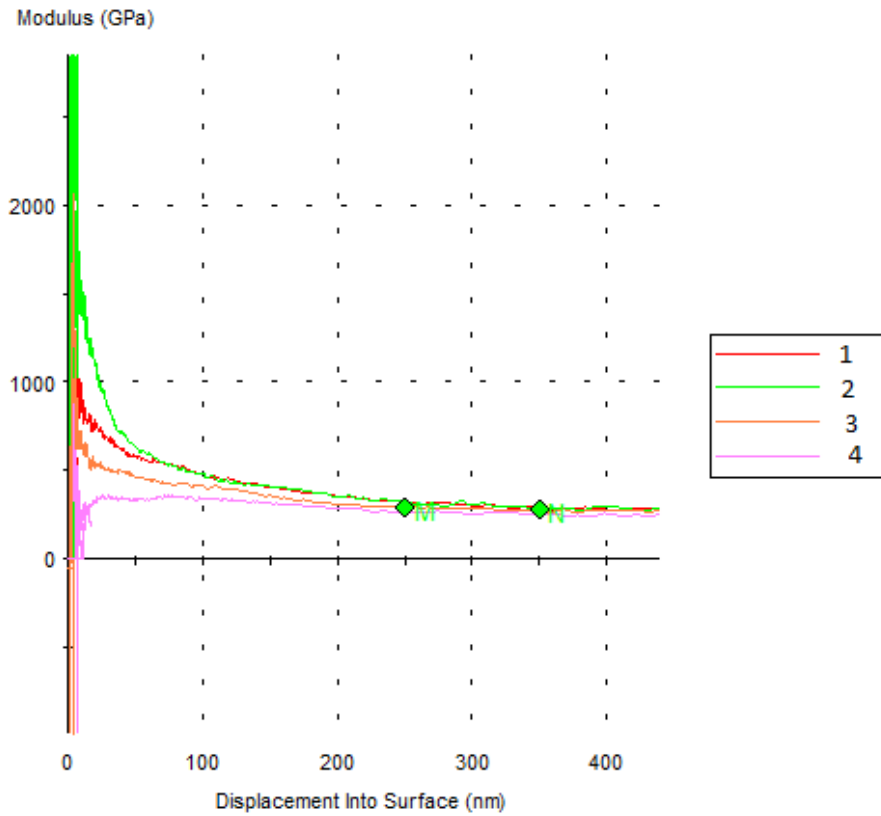


Fig 20 Youngs Modulus vs Displacement Curve

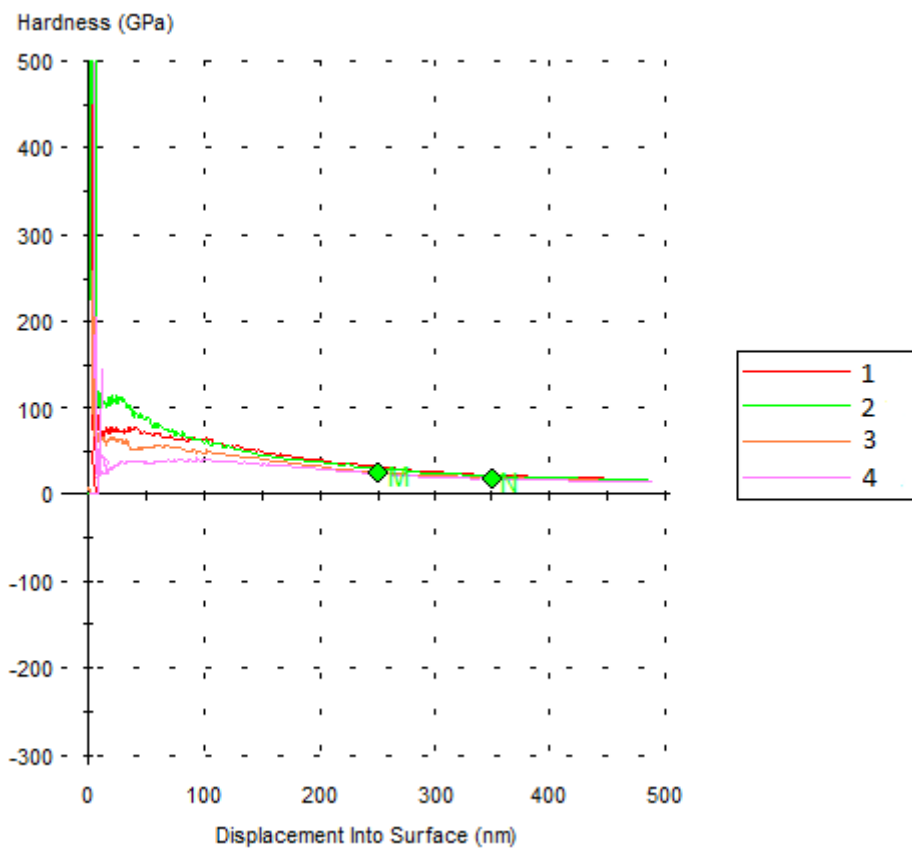


Fig 21 Hardness vs Displacement Curve

Table 2 Nanoindentation data

Test no.	Avg modulus (200–300 nm) (GPa)	Avg hardness (200–300 nm) (GPa)	Drift correction (nm/s)	Temperature (°C)
1	333.6	34.65	-0.050	25.2
2	335.6	32.86	-0.065	25.2
3	281.3	21.61	-0.064	25.1
4	271.7	26.07	-0.102	25.0
Mean	305.6	28.8	-0.079	25.1

3.5.3 Surface Roughness

The surface roughness of the specimen was determined before and after the DLC coating using TALYSURF, a high resolution rugosimeter equipment. Table 3 shows the obtained surface roughness values. The results in table 3 show that there is good agreement between the pre coating and post DLC coating surface roughness values. There was a decrease of 5.76% in the average surface roughness values post DLC coating.

Table 3 Surface roughness

Specimen	Trial	R _a (Average roughness) [nm]	R _a (Average roughness) (average of trials) [nm]
Substrate material HSS M2 (polished)	1	19.3	19.2
	2	19.1	
HSS M2/DLC	1	16	16.1
	2	16.2	

3.5.4 Raman Spectroscopy

Raman spectroscopy of the as-deposited DLC coatings was performed on a Raman spectrometer at a wavelength of 532 nm wavelength. The Raman spectra of the coating display a broad Raman band from 1150 cm⁻¹ to 1700 cm⁻¹, along with peaks at 1528 cm⁻¹ and 1375 cm⁻¹ called the G-peak and D-peak, respectively. These peaks show changes in position and intensity based upon the structural changes.

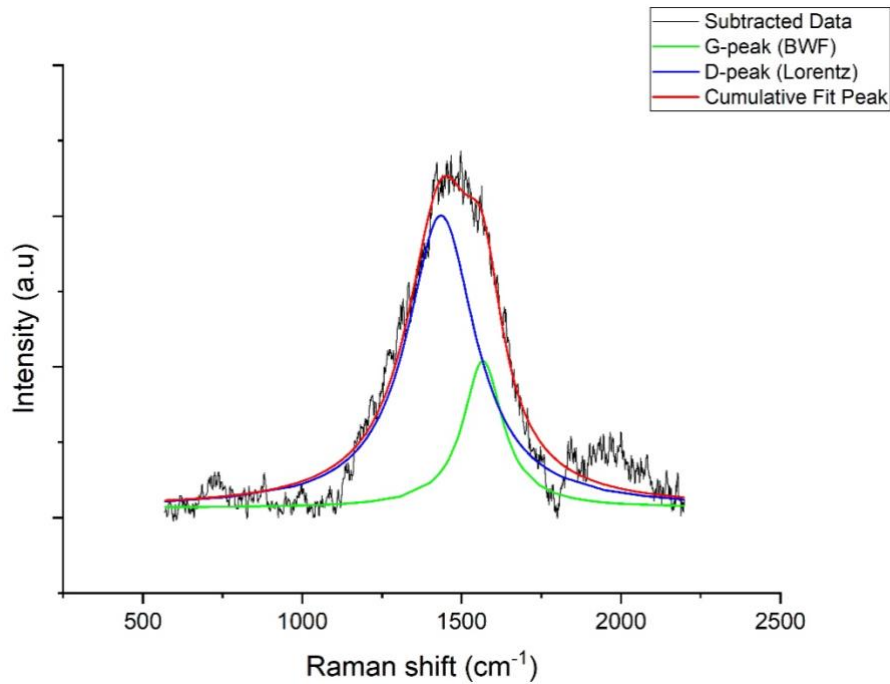


Fig. 22 Raman spectra of as-deposited DLC at 514 nm wavelength

Table 3. Information deduced from the Raman data after peak de-convolution.

Wavelength (nm)	D peak position (cm ⁻¹)	G peak position (cm ⁻¹)
514	1435	1566.95

Fig 22 shows the Raman peak shifts obtained using micro-Raman spectroscopy (Seiko Technotron STR 300 model) emitting laser at 514 nm wavelength. The Raman G- peak and D- peak were identified using BWF function and Lorentzian function respectively defined in, as suggested by Ferrari et al. [20]. Background noise for Raman spectrum was removed using second derivative adjacent-averaging smoothing method in Origin Pro 2019 b software. Spline interpolation method was used to define the baseline for the Raman spectrum.

3.5.5 Critical load and coefficient of friction

A typical Displacement – scratch distance curve indicating the critical load for DLC coated at 250 V and 100 sccm is as shown in figure 23. Critical load for DLC coated substrates was 123.99mN. The variation of COF along the scratch distance for all experimental conditions along with uncoated substrate is as shown in Figure 24. The coefficient of friction of DLC coated steel is found to be 0.07 as compared to as received HSS M2 steel which was 0.17. Clearly, the coefficient of friction is related to crystal phases of carbon and percentage of carbon content in DLC. Increase in coefficient of friction can be attributed to the decrease of amorphous carbon content and self-lubrication property.

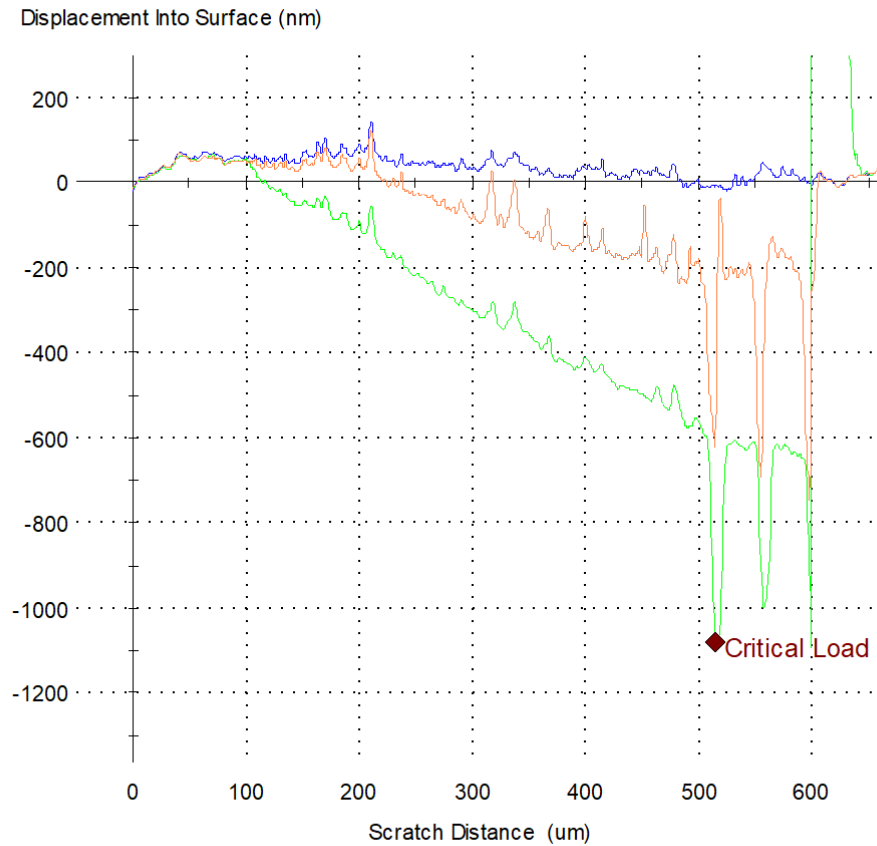


Fig. 23 Displacement vs scratch distance

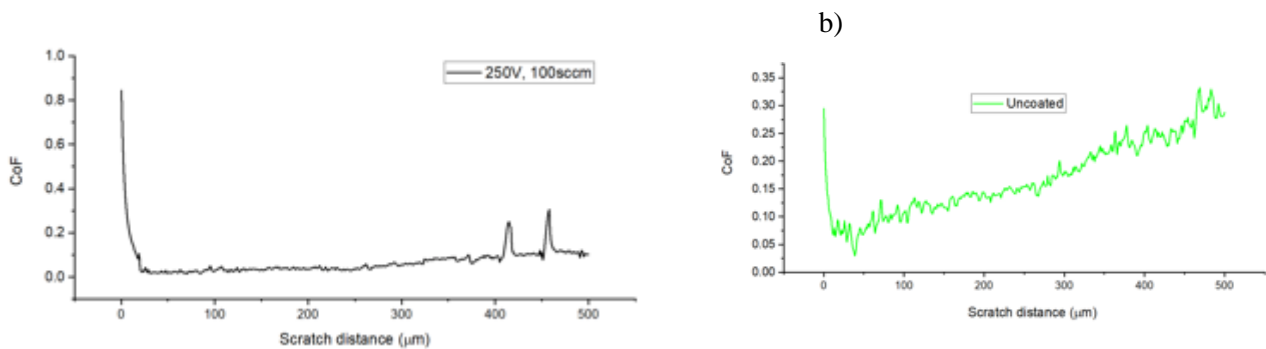


Fig. 24 COF vs scratch distance a) DLC coated b) Uncoated HSS M2

Conclusion

The effect of DLC-coated HSS M2 steel slid against 20MnCr20 steel disk was modeled using ANSYS 18.1 finite element analysis code. The effect of normal load on tribological and structural responses was analyzed to explore the performance of DLC coatings in hydraulic applications. The wear volume was significantly reduced for DLC-coated pin at higher normal loads because of lower elastic modulus mismatch between the

substrate and coating. Also, decrease in contact pressure was achieved due to reduced heat generation at the interface because of enhanced heat dissipation by DLC coating. Frictional contact stresses for the DLC-coated pin decreased by 56.21% on an average for all the load conditions when compared with as-received HSS M2 pin since a higher degree of graphitization resulted in lower shear resistance of contact asperities.

Acknowledgment

This research did not receive any specific grant from funding agencies in the public, commercial, or not-for-profit sectors.

Conflict of interest statement

On behalf of all the authors, AB—the corresponding author—states that there is no conflict of interest.

REFERENCES

- [1] Marin E, Lanzutti A, Nakamura M et al (2019) Corrosion and scratch resistance of DLC coatings applied on chromium molybdenum steel. *Surf. Coatings Technol.* 124944.
- [2] Masripan NA Bin, Ohara K, Umehara N et al (2013) Hardness effect of DLC on tribological properties for sliding bearing under boundary lubrication condition in additive-free mineral base oil. *Tribol Int* 65:265–269. <https://doi.org/10.1016/j.triboint.2013.01.016>
- [3] Konkhunthot N, Tunmee S, Zhou XL et al (2018) The correlation between optical and mechanical properties of amorphous diamond-like carbon films prepared by pulsed filtered cathodic vacuum arc deposition. *Thin Solid Films* 653:317–325. <https://doi.org/10.1016/j.tsf.2018.03.053>
- [4] Wu Y, Liu JQ, Cao HT et al (2020) On the adhesion and wear resistance of DLC films deposited on nitrile butadiene rubber: A Ti-C interlayer. *Diam Relat Mater* 107563. <https://doi.org/10.1016/j.diamond.2019.107563>
- [5] Jin X, Zhang Y, Chen L et al (2018) Preparation and tribological behaviors of DLC/spinel composite film on 304 stainless steel formed by cathodic plasma electrolytic oxidation. *Surf. Coatings Technol* 338:38–44. <https://doi.org/10.1016/j.surfcoat.2018.01.069>
- [6] Lu Y, Huang G, Xi L (2019) Tribological and mechanical properties of the multi-layer DLC film on the soft copper substrate. *Diam Relat Mater* 94:21–27. <https://doi.org/10.1016/j.diamond.2019.02.019>
- [7] Łępicka M, Grądzka-Dahlke M, Pieniak D et al (2017) Effect of mechanical properties of substrate and coating on wear performance of TiN- or DLC-coated 316LVM stainless steel. *Wear* 382–383:62–70. <https://doi.org/10.1016/j.wear.2017.04.017>
- [8] Duminica FD, Belchi R, Libralesso L, Mercier D (2018). Investigation of Cr(N)/DLC multilayer coatings elaborated by PVD for high wear resistance and low friction applications. *Surf. Coatings Technol* 337:396–403. <https://doi.org/10.1016/j.surfcoat.2018.01.052>
- [9] Kim DW, Kim KW (2014) Effects of sliding velocity and ambient temperature on the friction and wear of a boundary-lubricated, multi-layered DLC coating. *Wear* 315(1-2):95–102. <https://doi.org/10.1016/j.wear.2014.04.002>
- [10] Ma Q, Wang X, Yuan F et al (2016) Effects of the friction coefficient on the torque characteristics of a hydraulic cam-rotor vane motor. *J Mech Sci Technol* 30(8):3507–3514. <https://doi.org/10.1007/s12206-016-0710-8>
- [11] Inaguma Y, Hibi A (2005). Vane pump theory for mechanical efficiency. *Proc Inst Mech Eng Part C J Mech Eng Sci.* 219(11):1269–1278. <https://doi.org/10.1243/095440605X32002>
- [12] Inaguma Y (2010) Reduction of friction torque in vane pumps by using physical vapour deposition-coated vane. *Proc Inst Mech Eng Part C J Mech Eng Sci.* 224(11):2449–2458. <https://doi.org/10.1243/09544062JMES2120>
- [13] Ashmawy M, Murrenhoff H (2009) Experimental investigation of friction force between vane tip and cam-ring in oil vane pumps. *Int J Fluid Power* 10(1):37–46. <https://doi.org/10.1080/14399776.2009.10780966>
- [14] Pandure PS, Jatti VS, Singh, TP (2014) Finite Element Simulation of Nano-indentation of DLC Coated HSS Substrate. *Procedia Mater Sci* 6:1619–1624. <https://doi.org/10.1016/j.mspro.2014.07.145>

- [15] Suresh R, Kumar MP, Basavarajappa S et al (2017) Numerical Simulation & Experimental study of wear depth and Contact pressure distribution of Aluminum MMC Pin on Disc Tribometer in: Materials Today Proceedings. Elsevier Ltd, pp. 11218–11228. <https://doi.org/10.1016/j.matpr.2017.09.043>
- [16] Holmberg K, Ronkainen H, Laukkanen A et al (2006) Tribological analysis of TiN and DLC coated contacts by 3D FEM stress modeling and fracture toughness determination, in: VTT Symposium (Valtion Teknillinen Tutkimuskeskus) pp.311–328.
- [17] Li H (2012) FEA Modeling of a Tribometer's Pin and Disk Interaction. Dissertation, McMaster University
- [18] Söderberg A, Andersson S (2009) Simulation of wear and contact pressure distribution at the pad-to-rotor interface in a disc brake using general purpose finite element analysis software. Wear 267(12):2243–2251. <https://doi.org/10.1016/j.wear.2009.09.004>
- [19] Oliver WC, Pharr GM (2004) Measurement of hardness and elastic modulus by instrumented indentation: Advances in understanding and refinements to methodology. J Mater Res 19(1):3–20. <https://doi.org/10.1557/jmr.2004.19.1.3>
- [20] Ferrari AC (2002) Determination of bonding in diamond-like carbon by Raman spectroscopy. Diam Relat Mater 11(3-6):1053–1061. [https://doi.org/10.1016/S0925-9635\(01\)00730-0](https://doi.org/10.1016/S0925-9635(01)00730-0).
- [21] Varade A, Niranjana Reddy K, Saseen D et al (2014). Detailed Raman study of DLC coating on Si (100) made by RF-PECVD. Procedia Engineering. Elsevier Ltd 1452–1456. <https://doi.org/10.1016/j.proeng.2014.12.428>
- [22] Holmberg K, Mathews A (2009) Coatings Tribology properties, mechanisms, techniques and applications in surface engineering. First edition, Elsevier. UK.
- [23] Gabriel HM, Schmidt F, Broszeit E, Kloos, KH (1983) Improved component performance of vane pumps by ion-plated TiN coatings. Thin Solid Films 108(2):189–197. [https://doi.org/10.1016/0040-6090\(83\)90504-7](https://doi.org/10.1016/0040-6090(83)90504-7)
- [24] Mishra D, Sonia FJ, Srivastava D et al (2018) Wear damage and effects of graphene-based lubricants/coatings during linear reciprocating sliding wear at high contact pressure. Wear 400–401:144–155. <https://doi.org/10.1016/j.wear.2017.12.024>
- [25] Kim DW, Kim KW (2011) Friction and wear characteristics of diamond-like carbon (DLC) coating used for machine elements. American Society of Mechanical Engineers, Tribology Division, TRIB. 203–205. <https://doi.org/10.1115/IJTC2011-61071>